HYDROLOGICAL PROCESSES

Vol; 18

Page; 23 -39

Published; January 2004

Hydrometeorological behaviors of pine and larch forests in eastern Siberia

Shuko HAMADA[1, 2], Takeshi OHTA[2, 3], Tetsuya Hiyama[4], Takashi KUWADA[5], Atsuhiro TAKAHASHI[6], and Trofim. C. MAXIMOV[7]

[1]*Graduate School of Agriculture, Iwate University, Morioka 020-8550, Japan*

[2]*Graduate School of Bioagricultural Sciences, Nagoya University, Nagoya 464-8601, Japan*

[3]*Frontier Observational Research System for Global Change, Yokohama 236-0001, Japan*

[4]*Institute of Hydrospheric-Atmospheric Sciences, Nagoya University, Nagoya 464-8601, Japan*

[5]*Graduate School of Natural Science and Technology, Okayama University, Okayama 700-8530, Japan*

[6]*Graduate School of Science, Nagoya University, Nagoya 464-8601, Japan*

[7]*Institute for Biological Problems of the Cryolithozone, Siberian Division of Russian Academy of Sciences, Yakutsk 677891, Russia*

Address for correspondence: Takeshi OHTA

Graduate School of Bioagricultural Sciences,

Nagoya University,

Furo-cho, Chikusa-ku, Nagoya 464-8601, Japan

Tel. & Fax: +81-52-789-4059

E-mail: takeshi@agr.nagoya-u.ac.jp

Abstract

Seasonal changes in the water and energy exchanges over a pine forest in eastern Siberia were investigated and compared with published data from a nearby larch forest. Continuous observations (April to August 2000) were made of the eddy-correlation sensible heat flux and latent heat flux above the canopy. The energy balance was almost closed, while the sum of the turbulent fluxes sometimes exceeded the available energy flux (R_n-G) when the latent heat flux was large; this was related to the wind direction. We examined the seasonal variation in energy balance components at this site. The seasonal variation and magnitude of the sensible heat flux (H) was similar to that of the latent heat flux (λE), with maximum values occurring in mid-June. Consequently, the Bowen ratio was around 1.0 on many days during the study period. On some clear days just after rainfall, λE was very large, and the sum of H and λE exceeded R_n-G. The evapotranspiration rate above the dry canopy from May to August was 2.2 mm·day^{-1}. The contributions of understory evapotranspiration (E_u) and overstory transpiration (E_o) to the evapotranspiration of the entire ecosystem (E_t) were both from 25 to 50% throughout the period analyzed. These results suggest that E_u plays a very important role in the water cycle at this site. From snowmelt through the tree growth season (23 April to 19 August 2000), the total incoming water, comprised of the sum of precipitation and the water equivalent of the snow at the beginning of the melt season, was 228 mm. Total evapotranspiration from the forest, including interception loss and evaporation from the soil when the canopy was wet, was 208-254 mm. The difference between the incoming and outgoing amounts in the water balance was from +20 to -26 mm. The water and energy exchanges of the pine and larch forest differed in that λE and H increased slowly in the pine forest, while λE increased rapidly in the larch forest and H decreased sharply

after the melting season. Consequently, the shape of the Bowen ratio curves at the two sites differed over the period analyzed, as a result of the differences in the species in each forest and in soil thawing.

Key words: Water and energy exchanges, SVAT, Understory evapotranspiration, Bowen ratio, eddy correlation, GAME-Siberia, GEWEX

Introduction

The circumpolar northern boreal forest extends south of 70°N in Siberia, and north of 50°N in Mongolia, adjacent to southeast Siberia, and south of Hudson Bay in eastern Canada (Larsen, 1980). This vast boreal forest covers about 900 million ha between 50 and 70° North, and the Siberian boreal forest accounts for 70% of the total. The interaction between the land surface and atmosphere has been identified as one of the most important processes in climate studies (*e.g.*, Betts *et al.*, 1996). Therefore, to clarify the mechanisms of global climate change it is important to understand the characteristics of the water and energy cycles of this vast area of forest.

Recently, several studies have examined water and energy cycles in boreal forests. Long-term observations of water and energy exchanges have been carried out in northern Canada as part of international projects such as the Boreal Ecosystem-Atmosphere Study (BOREAS), in order to better understand interactions between the boreal forest biome and the atmosphere (Sellers *et al.*, 1995, 1997). The daily evapotranspiration rates were usually less than 1.5 $mm \cdot day^{-1}$ during the growing season in Canadian boreal forest conifers, but the rate was dependent on whether the canopy was wet (Baldocchi *et al.*, 1997). In an aspen forest, most of the available energy flux was converted to sensible heat flux before leaf emergence, while after leaf emergence latent heat flux dominated (Blanken *et al.*, 1997). Coniferous vegetation was characterized by a low evaporative fraction in comparison with deciduous forest (Sellers *et al.*, 1997).

The Northern Hemisphere Climate-Processes Land-Surface Experiment (NOPEX) project was initiated in the southern Scandinavian boreal zone in central Sweden (Halldin *et al.*, 1999). Here, pine and spruce trees transpired differently,

especially in spring. Long-term measurements of sap flow in a mixed pine-spruce forest showed that drought affected transpiration by pines less than that by spruce (Cienciala *et al*., 1999).

Interest in the energy and water cycles in Siberian boreal forests has been growing, and some studies have been made. In eastern Siberia, mid-summer observations found that the daily mean evapotranspiration was 1.9 mm·day^{-1} in a larch forest (Kelliher *et al*., 1997) and 0.8-2.3 mm·day^{-1} in a central Siberian pine forest (Kelliher *et al*., 1998); in the pine forest, the evaporation rates were regulated largely by rainfall. In humid regions, such as Japan, evapotranspiration is approximately 3.4 mm·day^{-1} in evergreen coniferous forest (Hattori *et al*., 1993) and 3.1 mm·day^{-1} in deciduous broad-leaved forest (Tamai *et al*., 1996), so the evapotranspiration in Siberian boreal forests is about 60% of that in Japan.

Long-term observations in an eastern Siberian boreal forest began in 1996 as part of the GAME (GEWEX Asia Monsoon Experiment)-Siberia project. As a result, the characteristics of the water and energy cycles in a larch forest during the growing season, from snowmelt to the leaf-fall season, have been determined. The seasonal change in the Bowen ratio over forests appears ‘U’-shaped, and the lowest values, about 1.0, occur in June and July. Understory evapotranspiration is high, comprising about 35% of the evapotranspiration of the entire ecosystem, because the canopy is sparse and the leaf area index is low (Ohta *et al*., 2001a). Understory evapotranspiration is therefore a major contributor to the overall exchange of mass and energy.

There is still, however, a need for long-term observations and analysis to better understand the water and energy exchanges. Especially, few studies have examined

seasonal changes for different tree species in Siberia. The objectives of this paper were 1) to clarify seasonal changes in the energy and water cycles in a Siberian evergreen forest; 2) to examine the relationship between the total evapotranspiration of the ecosystem and understory and overstory transpiration; and 3) to clarify differences in the properties of the energy and water cycles in evergreen (pine) and deciduous (larch) forests.

Methods

Site description

Pine site

The study site was a pine forest (*Pinus sylvestris*) at Spasskaya Pad (62°14'29" N, 129°39'2" E), located about 20 km north of Yakutsk in eastern Siberia. This site is located in a continuous permafrost region at an altitude of 220 m a.s.l.; the permafrost front reaches the surface during winter, and the active layer is about 2.5 m deep in summer. The stand studied was about 600 m by about 2 km, and was surrounded by a larch forest (*Larix gmelinii*) containing some birch (Figure 1). The topography of the area is flat, with an inclination of 2~3 degrees. According to GRID Global Data (IIASA Climate - mean monthly precipitation and mean monthly temperature), the mean annual temperature is -10.2 °C and the annual precipitation is 188 mm.

The average tree height at the study site was about 10 m, although it was only 2 m in some areas. Figure 2 (a) shows a crown projection diagram for this site. The dots and circles indicate the positions of pine trunks and the spread of the canopy, respectively, and dark color shows understory vegetation. The stand density was 2,660 trees ha^{-1}, and the average trunk diameter at breast height (*DBH*) was 7.9 cm including values of thin trees.

The understory vegetation was mainly cowberry (*Vaccinium uva ursi*). The plant area index (*PAI*) of the tree canopy, which was obtained from an analysis of fish-eye photographs, was 2.5 (Toba and Ohta, 2001). The leaf area index (*LAI*) of the cowberry was 2.5. This result was obtained by sampling cowberry in 10 plots (0.1 × 0.1 m). *LAI* is the total one-side leaf area per unit ground surface area and *PAI* contained not only leaves but also trunks and branches. The cowberry was located mainly where short trees stood close together.

Larch site

The larch site is located at 62°15'18" N, 129°37'8" E, in the reaches of Lena river, where is continuous permafrost region, and the active layer is about 1.2 m deep. A 32 m tower was installed in the larch forest; about 2.5 km northwest of the pine site, and observations of turbulent fluxes and meteorological factors began there in September 1996 (Ohta *et al*., 2001a). The altitude is 220 m a.s.l. The main species of tree is Dahurica larch (*Larix gmelonii*), with a stand density of 840 trees ha^{-1}. The mean stand height is 18 m. Figure 2 (b) shows a crown projection diagram for this site. Understory trees are mainly *Betula platyphylla*. The value of *PAI* varied between 3.71 in the foliated season and 1.71 in the leafless season. The *PAI* was obtained from analysis of fish-eye photographs and confirmed by litter fall observations. Understory vegetation is cowberry (*Vaccinium uva ursi*). Its leaf density is high, but the *PAI* (or *LAI*) was not measured (Ohta *et al*., 2001a).

The measurements

Pine site

An 18.2-m-high observation tower was installed at the center of the pine forest in September 1999. Most measurements were made continuously from April to September 2000. Turbulent fluxes above the canopy were measured at a height of 19.1 m using the eddy correlation method. The sensible and latent heat fluxes were measured using a three-dimensional ultrasonic anemo-thermometer (KAIJO, DA-600) and an open path H_2O gas analyzer (KAIJO, AH-300), respectively. The output from these instruments was recorded using a data logger (TEAC, DR-M3) at a sampling rate of 10 Hz.

Downward and upward of long-wave radiation above the canopy were measured using radiometers (Eiko, MS-201F) at 18.2 and 15.9 m, respectively. The long-wave radiation data were corrected using the temperature sensed at domes and sensor bodies. Downward and upward of short-wave radiation above the canopy were also measured with radiometers (Kipp & Zonen, CM-6F) at 18.2 and 15.9 m, respectively. The net all-wave radiation above the canopy was derived from the sum of the four radiation components. When these data were lacking, we used data obtained from a net radiometer (REBS, Q7) at 15.9 m. On the forest floor, downward and upward short-wave radiation were measured using pyranometers with silicon photo diodes, and net all-wave radiation was measured using a net radiometer (REBS, Q7) at 1.4 m. Radiation was measured at a relatively homogeneous location at exactly 1-min intervals, and 5-min average values were recorded using data loggers (GRANT, SQ-1209; Hakusan, LS-3300). Air temperature and relative humidity were measured using humicap sensors (VAISALA, HMP-350) at 17.2 and 13.4 m. Wind speed was measured with three-cup anemometers (Makino, AC-750) at 18.2, 13.8, 12.2, and 1.9 m, and wind direction was measured

(Makino, WS-104) at 18.2 m. The data were recorded at 5-minute intervals using data loggers (GRANT, SQ-1209; Hakusan, LS-3300).

Ground temperatures were measured with thermistors at six depths (0, 0.1, 0.2, 0.4, 0.8, and 1.2 m) at 30-min intervals, and soil moisture was measured with a tensiometer at five depths (0.1, 0.2, 0.4, 0.8, and 1.2 m) every other day. Precipitation was measured using a tipping-bucket rain gauge with 0.125-mm resolution, and recorded using a data logger every 5 minutes (Kona System, KADEC-UP) at an open site 1.6 km west of the observation tower (Figure 1). In the pine forest, throughfall was measured using ten plastic gutters, each 2 m long and 0.2 m wide, and stem flow was measured with six trees (Toba and Ohta, 2001).

The understory evapotranspiration was estimated by weighing two lysimeters, each 0.165 m in diameter and 0.075 m deep, containing undisturbed soil samples, which were left out for about 24 hours. The understory evapotranspiration was measured approximately every 10 days. The soil samples with vegetation were refreshed at the start of each experiment. The two pans were weighed in the morning on two consecutive days.

To estimate the rate of transpiration from pine trees, four sample trees were selected that represented a range of *DBH*, and the sap flow velocity of these trees was measured using the heat pulse method. The *DBH* of the sample trees was 0.083, 0.134, 0.154, and 0.205 m. Heat pulse velocity data were recorded every 10 minutes using a data logger (Hakusan, LS-3300) (Marshall, 1958).

During the snowmelt season, we observed the snow ablation process. The density of the entire snow layer in a cylinder and the spatial averaged snow depth were measured and used to calculate the water equivalent of the snow pack. These measurements were

carried out manually from 18 April to 1 May. The times of the observations were generally 0600, 1400, and 2000.

Larch site

A 32-m-high observation tower was installed in the larch forest in the autumn of 1996, and preliminary observations began at the beginning of September 1996. More detailed observations were started in the middle of August 1997.

An ultrasonic anemometer (KAIJO, DA-600) operated every 15 min and measured the three-dimensional wind speed and air temperature for 13.667 min at 10 Hz. A water vapour analyzer with closed path (Li-COR, LI-6262) operated intermittently at 10 Hz. The four components radiation and the net all-wave radiation above the canopy were measured every minute, and recorded at 5-minute intervals. The ground heat flow was measured with a heat plate (Eiko, MF-81) at 0.05 m depth.

Ground temperatures and soil moisture were measured with thermistors at seven depths at 5-min intervals. The understory evapotranspiration was estimated with the same two pans as the pine site. The pans were every 2 h in the daytime; they were not weighed at night. The measurements were carried out every 5 days (For details, see Ohta *et al*., 2001a).

Data analysis

The energy balance above a forest canopy can be described as follows:

$$R_n = H + \lambda E + G + J \quad (1)$$

where R_n is the net all-wave radiation ($W \cdot m^{-2}$), H is the sensible heat flux ($W \cdot m^{-2}$), λE is the latent heat flux ($W \cdot m^{-2}$), G is the ground heat flow ($W \cdot m^{-2}$), and J is the change in heat

storage in the canopy layer ($W \cdot m^{-2}$). Since we did not measure *J*, we regard *J* as 0 when we discuss the energy balance using hourly data. When the daily energy balance is discussed, *J* is ignored, since storage of heat during the daytime is cancelled by the energy released at night.

The turbulent fluxes above the canopy were measured using the eddy correlation technique. The basic equations for *H* and λE can be written as follows:

$$H = \rho C_p (\overline{w't'}) \quad (2)$$

$$\lambda E = \lambda \rho (\overline{w'q'}) \quad (3)$$

$$w' = w - \overline{w} \quad (4)$$

$$t' = t - \overline{t} \quad (5)$$

$$q' = q - \overline{q} \quad (6)$$

where ρ and C_p are the air density ($kg \cdot m^{-3}$) and specific heat of air at a constant pressure ($J \cdot kg^{-1}K^{-1}$), respectively, and *w*, *t*, and *q* are the vertical component of wind speed ($m \cdot sec^{-1}$), air temperature (°C), and specific humidity ($kg\ kg^{-1}$), respectively. The primes indicate the instantaneous deviation from the mean, and the overbars indicate temporal averages. The data were measured at a frequency of 10 Hz, and calculations were made every 29.5 minutes. Three-angle coordinate rotation was calculated to make the average vertical wind speed zero. Other corrections were not made.

The ground heat flow (*G*) in the pine forest was estimated by a calorimetric method using soil temperature profiles (Kimball *et al.*, 1975). *G* was calculated as follows:

$$G = \sum_{i=1}^{m} q_i + q_b \quad (7)$$

$$q_i = C_i \cdot \Delta x_i \cdot \Delta\theta_i / \Delta t \quad (8)$$

where q_i is the change in heat content per unit time ($W \cdot m^{-2}$), q_b is the change in heat content per unit time at a depth of b ($W \cdot m^{-2}$), C_i is the volumetric heat capacity of the i^{th} layer ($J \cdot m^{-3} K^{-1}$), Δx_i is the thickness of the layer (m), and $\Delta\theta_i / \Delta t$ is the hourly temperature change ($K \cdot hr^{-1}$). G was calculated by adding q_i until q_b was near zero. In this study, ground temperatures were measured at six depths (0, 0.1, 0.2, 0.4, 0.8, and 1.2 m). We calculated G using the data from 0 to 0.4 m depth, because there was a clear daily variation in this layer. As soil moisture was not measured continuously, we used the value of C_i that was obtained at a depth of 0.1 m in another pine forest site, near this site. C_i was regarded as constant in all layers, and was fixed at 1.3×10^6 $J \cdot m^{-3} K^{-1}$.

To estimate overstory transpiration, we correlated sap flow to the average trunk *DBH* and applied this correlation to every stand for 50 × 50-m squares surrounding the tower. The experimental relationship between the measured sap flow and *DBH* (cm) is given by

$$V = a \times DBH^b \quad (9)$$

where V is the amount of sap flow ($L \cdot day^{-1}$), and a and b are coefficients. The values of a and b were determined from the daily relationship obtained from the four sample trees.

In this study, the interception loss was calculated by subtracting the sum of stem flow and throughfall from precipitation which was measured at the open site (See, Figure 1). At this site, the relationship between throughfall or stem flow and precipitation can be approximated by the following linear functions (Toba and Ohta, 2002):

$$T = 7.6\times10^{-1}P - 3.9\times10^{-1} \quad (10)$$

$$S = 1.1\times10^{-3}P - 3.4\times10^{3} \quad (11)$$

where T is throughfall (mm), S is stem flow (mm), and P is the gross precipitation at the open site (mm). For days when there were no throughfall or stem flow data, the values were estimated using these equations. It was reported that the correlation coefficient (r^2) of the equation (10) and (11) was 0.94 and 0.59, respectively (Toba and Ohra, 2002). These results suggest that throughfall can be estimated well because there is a close relation between throughfall and the gross precipitation. On the other hand, the range of r^2 between stem flow and gross precipitation was low, but the amount is very small and the error is negligible.

Results and discussion

Meteorology

Figure 3 shows the seasonal variation in the meteorological variables. These variables are expressed as daily mean values, except for precipitation. There was snow cover during winter, which melted between 19 April and 3 May, 2000. The albedo above the canopy was about 0.5 when there was snow cover, and dropped to about 0.2 after the snow melted. There were clear seasonal variations in air temperature and short-wave radiation. The total precipitation observed at the open site was 145 mm from 27 April to 5 September 2000, 106 mm from 21 April to 7 September 1998 (Ohta *et al*., 2001a), and 236 mm from May to September 1999 (Ohta *et al*., 2001b). According to the GRID Global Data (IIASA Climate - Mean Monthly Precipitation), the average amount of precipitation from April to August is 146 mm. Therefore, the amount of precipitation during the period analyzed was normal. The maximum daily mean air temperature during

the measurement period was 25.2 °C, on 20 July, and the minimum was -2.6 °C, on 4 May. The amount of solar radiation reaching the ground at the study site was equal to 40 % of that above the canopy during the study period.

Turbulent fluxes

To examine the source area of turbulent fluxes, we analyzed the flux footprint using a footprint estimation model (Horst and Weil, 1992, 1994). The frequency was calculated at 2-m intervals. Figure 4 shows the correlation between the upwind distance and frequency distribution in the flux footprint. Each figure presents a typical daytime footprint for different atmospheric stabilities at a height of 19.1 m. We thought that it was important to know the flux source area in daytime, when a lot of heat and water are exchanged, but the flux at night was neglected in this study because it was usually small (For example, see Figure 9.). The upwind distance of the peak footprint was 20 m on 8 July, 24 m on 10 July during unstable conditions, and 36 m on 20 June during near-neutral conditions.

From May until the end of August, 80% of the total flux under unstable conditions came from 408 m, on average. In contrast, the source area was enlarged and it extended to 900 m under near-neutral conditions. Therefore, it is thought that in unstable conditions a large part of the source area was located within the pine stand. During near-neutral conditions, it seemed to extend beyond the study stand in some directions, although this was minimal in the daytime. Therefore, we believe that the following discussion of the characteristics of the pine forest is valid.

Energy balance

The energy balance was examined to confirm the quality of the observations. Figure 5 shows a test for closure of the energy balance using hourly data. The available energy flux, R_n-G, was generally in agreement with the sum of the turbulent fluxes, but when the available energy flux was large, the sum of the turbulent fluxes was often larger than the available energy flux. On average, the sum of the turbulent fluxes accounted for 101% of the available energy flux. We therefore examined the reason for this discrepancy in the energy balance.

Figure 6 shows the correlation between the bias in the energy balance, ($H+\lambda E$)-(R_n-G), and the sensible and/or latent heat fluxes. This figure shows that the latent heat flux has a strong effect on the bias in the energy balance. In contrast, there is no relationship between the sensible heat flux and the bias. Recently, disparities in the energy budget have been reported elsewhere. In many cases, it has been reported that the sum of the turbulent fluxes was underestimated compared with the available energy flux (*e.g.*, Lee and Black, 1993; Kelliher *et al*., 1997). In the larch forest at Spasskaya Pad, turbulent fluxes accounted for 75% of the available energy flux (Ohta *et al*., 2001a). At the pine site, however, the opposite result was obtained.

Figure 7 shows the bias in the energy balance as a function of wind direction for each 30° class. The error bars show 95% confidence intervals. This analysis used hourly data. The vertical axis in the top figure is the bias in the energy budget, ($H+\lambda E$)-(Rn-G), and the closure rate, ($H+\lambda E$)/(Rn-G). For wind directions between 240 and 330°, the sum of the turbulent fluxes exceeds the available energy flux, and the maximum bias occurs at 270°. Similarly, the closure rate increases and reaches 2.0 at 300°. At the same time, the

latent heat flux is also maximal (see the bottom figure). In contrast, for wind directions between 90 and 150°, the turbulent fluxes are smaller than the available energy, but there are no clear changes in the closure rate. These results show that wind direction affects the bias in the energy balance. Between 240 and 330° (west and north west), where the sum of the turbulent fluxes exceeds the available energy flux, the pine forest was about 300 m from the towers. However, there is a larch forest around this site, and the surrounding vegetation or topography might have affected the results. Bosveld and Bouten (2001) obtained a similar result for a Douglas-fir forest in the Netherlands, and indicated that wind direction affected non-closure in the energy balance, and that this had been caused by differences in the vegetation around the observation site. The footprint analysis suggests that during unstable conditions in daytime, most of the turbulent flux came from within the pine forest. However, when daytime conditions were near neutral, the size of the source area was extended. The turbulent fluxes were often overestimated in near-neutral conditions, and the energy imbalance might have been affected by the larch forest around the study stand.

Seasonal variation in the energy balance

The seasonal changes in the daily energy balance components above the canopy are shown in Figure 8. The data for the net all-wave radiation (R_n) and the turbulent fluxes for rainy days were excluded. The value of R_n increased in May and June. The maximum daily value of 190±10 $W \cdot m^{-2}$ occurred in the middle of June; which then decreased at the end of July and during August. The seasonal variation and magnitude of the latent heat flux (λE) were similar to those of the sensible heat flux (H); both were maximal in the

middle of June. Consequently, the Bowen ratio was around 1.0 on many days during the study period. In contrast, in the larch forest at Spasskaya Pad, the seasonal variation in the Bowen ratio was clearly 'U'-shaped (Ohta *et al*., 2001a). Therefore, the seasonal changes in the energy balance in the evergreen forest were quite different from those in the deciduous forest. On some clear days just after rainfall, λE was very large, and the sum of H and λE exceeded R_n. For example, on 22 June, the sum (376 $W \cdot m^{-2}$) of λE (199 $W \cdot m^{-2}$) and H (177 Wm^{-2}) greatly exceeded the net radiation (216 $W \cdot m^{-2}$), as also occurred on 1 May and 12 June. In a Canadian jack pine forest, the same phenomenon was seen; the highest λE was associated with clear days, just after significant rainfall events (Baldocchi *et al*., 1997).

Remarkably, from 7 to 22 July 2000, which corresponded to a long rainless period, λE decreased and was always smaller than H. Figure 9 shows the diurnal variation in the energy budget components during this period. The maximum hourly value of λE was about 240 $W \cdot m^{-2}$, on 8 July. However, the value gradually decreased, and the maximum λE was about 100 $W \cdot m^{-2}$ on 20 July, whereas R_n did not decrease. At the same time, the atmospheric saturation deficit gradually increased, and the maximum value (37.0 hPa) occurred on the last fine day (20 July). In contrast, there was no remarkable change in the suction (ψ) in the soil moisture, except at a depth of 0.1 m. The value of ψ was –117 cm H_2O at a depth of 0.1 m on 19 July, implying that it was slightly dry. These results suggest that λE was affected by the atmospheric saturation deficit rather than by soil moisture conditions.

Seasonal variation in evapotranspiration

Figure 10 shows the seasonal variation in the evapotranspiration above a dry canopy for the entire ecosystem (E_t), including overstory transpiration (E_o), and understory evapotranspiration (E_u). All the plots show daily values, and rainy days are excluded. E_t was determined using the eddy correlation method, and E_u was determined from lysimeter measurements. E_o was estimated from the sap-flow measurements using Eq. (9), where a ranged from 0.0371 to 0.212 and b ranged from 1.37 to 1.78. The value of r^2 between the amount of sap flow and *DBH* ranged from 0.944 to 0.981 and errors in the estimation of E_o considered to be small. The range of a was large in June and small in the middle of July and after the end of August. In contrast, the range of b showed the opposite tendency to a. It is thought that sap flow and the range of a decreased when a tree was strongly influenced by environmental variables. In addition, *DBH* might have an effect on the value of b.

E_t increased after the snowmelt in early May, reaching a maximum in June, and then decreasing in July and August. As mentioned above, E_t from eddy correlation measurements was very large on clear days just after rainfall. The highest value of E_t exceeded 6.0 mm·day^{-1}. Similar results were reported in a central Siberian pine forest (Kelliher *et al.*, 1998). E_t and E_o decreased remarkably during the rainless period in the middle of July, and increased after rainfall. The maximum daily E_u was 1.6 mm on 22 July. E_u increased in June, and the pattern was similar to the seasonal variation of E_t.

The daily mean value of E_t was 2.2 mm·day^{-1} from May to August. The average E_t during the summer (from July to the middle of August) was 1.7 mm·day^{-1}. We compared the average E_t at this site with values for other sites. Table 1 shows the daily mean

evapotranspiration rates (E_t) for Siberian and Japanese forests during the growing season. In Table 1, the results for Studies 1, 2, and 3 were determined by the eddy correlation technique and obtained under dry canopy conditions; Study 4 was estimated using his model and included values under dry and wet canopy conditions; and Studies 5 and 6 were estimated using the energy balance equation and the gradient method, respectively. In the larch forest at Spasskaya Pad (Study 2), the daily mean E_t in July and August 1999 was 1.5 mm·day^{-1} (Ohta *et al*., 2001a). A similar result was obtained at another Siberian site (Study 3) (Kelliher *et al*., 1997). The E_t at our site in Siberia was 60% of that in Japanese forests (Studies 5 and 6).

The relationships between E_t, E_u, and E_o are shown in Figures 11 and 12. Figure 11 shows the relationship between E_t and the sum of E_o and E_u, and that is similar to the larch site at Spasskaya Pad (Ohta *et al*., 2001a). At our study site, the sums of E_u and E_o almost agree with E_t. Figure 12 shows the relationships between E_t and E_u or E_o. E_u was 40-50% of E_t when E_t was small. When E_t exceeded 4 mm day^{-1}, the percentage of E_u dropped by about 25%. Similar results were obtained for E_o. Although the reason for this is not clear, it is possible that the spatial distribution of E_u was measured incorrectly because we used only two lysimeters. Comparing other Siberian sites, E_u was 35% of E_t during the growing season in the larch forest at Spasskaya Pad (Ohta *et al*., 2001a), while in another Siberian larch forest, E_u was 50% of E_t (Kelliher *et al*., 1997). Although the ratio of E_u to E_t differed in each stand, the daily E_t values in the three stands were similar. Consequently, the ratio of E_u to E_t may depend on the forest structure. It has been said that differences in transpiration between tree species are compensated for by transpiration from the understory vegetation (Roberts *et al*., 1982; Roberts, 1983). Our results show that differences in both tree species and in forest structure among the same species gave

similar results. As previously mentioned, the amount of solar radiation reaching the ground at the study site was equal to 40 % of that above the canopy. Therefore, it is thought that the potential E_u was high. These results suggest that E_u plays a very important role in the water cycle at this site.

Water balance

To examine the water balance at this site, we calculated the input and output water from snowmelt during the growing season. Snowmelt started in late April, and ended on 3 May. The water equivalent of snow on the first observation day was 85 mm. Precipitation from 23 April to 19 August 2000 totaled 143 mm. In this study, the interception loss was calculated by subtracting the sum of stem flow and throughfall from precipitation which was measured at the open site. For days when there were no throughfall or stem flow data, the values were estimated using equation (10) and (11); throughfall was 97 mm, and stem flow was less than 0.1 mm from 23 April to 19 August 2000. The interception loss was 46 mm during this period, or 30% of the precipitation at this site. The percentage precipitation interception loss at our study was two times larger than that at the larch forest (Ohta *et al*., 2001a). However, the evapotranspiration for the entire ecosystem from a wet canopy (E_w) is the sum of the evaporation of intercepted rainfall and the evaporation from the soil surface, and the latter could not be measured. As previously mentioned, when the canopy was dry, the overstory transpiration (E_o) and understory evapotranspiration (E_u) percentages of the evapotranspiration for the entire ecosystem (E_t) were the same. Therefore, we assumed that for understory evapotranspiration under rainy conditions: the minimum value was zero, and total evapotranspiration was 46 mm. The maximum values under a dry canopy would be the same percentage of total

evapotranspiration (50%). In this case, under rainy conditions the understory evapotranspiration was assumed to be 46 mm, and the total evapotranspiration would therefore be 92 mm. During this period, E_t calculated using the eddy correlation method exclusive of rainy days was 162 mm. Consequently, the total forest evapotranspiration, which is the sum of E_t and E_w, was estimated to be 208 – 254 mm (1.8-2.1 mm day^{-1}). In a central Siberian pine forest, the daily mean evapotranspiration calculated from short-term measurements and climatological data was 1.7 mm day^{-1} from May to September (Kelliher *et al*., 1998), which is less than at our study site. The monthly variation in E_t and (E_t+E_w) are shown in Figure 13. The error bar represents the maximum evaporation after considering the maximum understory evapotranspiration values assumed above. This figure shows that maximum evapotranspiration occurred in June.

From these results, the total incoming water, *i.e*., the sum of precipitation and the water equivalent of the snow, was 228 mm from 23 April to 19 August 2000, and total evapotranspiration from the entire ecosystem ranged from 208 to 254 mm, as above. The water balance ranged from -26 to +20 mm taking water output away from input.

Comparison of the water and energy exchanges in the pine and larch forests

There were significant differences in the water and energy exchanges of the pine and larch forests at Spasskaya Pad just after the snowmelt season. Figure 14 shows the seasonal variation in the energy balance components (Ohta *et al*., 2001a). The latent heat flux (λE) increased rapidly, and the sensible heat flux (H) decreased remarkably from the latter part of May to early June. As previously mentioned, however, λE and H in the pine forest increased slowly from May to early June. It is thought that this resulted from the

difference in tree species in the deciduous and evergreen forests. Transpiration should start more slowly at a larch site than at a pine site, because it takes some time for leaf emergence in a larch forest; larch trees can transpire actively only after leaf emergence. In addition, the soil began to thaw earlier at the pine site than in the larch forest; on 11 May 2000, the daily maximum soil temperature at a depth of 0.1 m was 12.5 °C at the pine site and -0.4 °C at the larch site (Ohta *et al*., 2001b). The pine trees were therefore able to use water in the soil to transpire earlier than the larch trees, which could also have contributed to the difference in the transpiration characteristics of the two sites. Consequently, the seasonal variation in the Bowen ratio at the pine site differed markedly from that at the larch site over the course of the period analyzed.

The daytime sap flow velocity was always higher in the larch forest than in the pine forest. As previously mentioned, the contribution of understory evapotranspiration (E_u) to the total evapotranspiration of the entire ecosystem (E_t) above a dry canopy was larger at the pine site than at the larch site. E_t was slightly larger over the pine forest. Therefore, it is thought that E_o under a dry canopy at the pine site was almost the same as, or larger, than at the larch site.

The rate of interception loss at the pine site was twice that at the larch forest from the time of snowmelt through the tree growing season. In contrast, the plant area index (*PAI*) at the pine and larch sites were 2.8 and 3.7, respectively, in the foliated season. Therefore, there was no relationship between the *PAI* and the interception loss.

Conclusions

Seasonal changes in the water and energy exchanges in an eastern Siberian

evergreen forest were investigated, and compared with results for a larch forest. The new interpretations obtained in this study are as follows:

1. The sum of the turbulent fluxes was generally in good agreement with the available energy flux, except when the latent heat flux was large, when the total turbulent fluxes often exceeded the available energy flux; this bias in the energy balance was affected by the wind direction. Although the reasons for this phenomenon at this site are not clear, it might be an effect of the larch forest surrounding the site.
2. The seasonal variation and magnitude of the latent heat flux (λE) were similar to those of the sensible heat flux (H); both were maximal in June. Consequently, the Bowen ratio was around 1.0 on many days during the study period. On some clear days just after rainfall events, λE was very large, and the sum of H and λE exceeded the net all-wave radiation.
3. Remarkably, from 7 to 22 July 2000, which corresponded to a long rainless period, λE decreased and was smaller than H. Considering the diurnal change in the saturation deficit and soil moisture for the same period, it is thought that λE was affected by the atmosphere rather than by the soil.
4. The contribution of understory evapotranspiration (E_u) to the evapotranspiration from the entire ecosystem (E_t) was 25-50% of E_t throughout the period analyzed, and a similar relationship was obtained for overstory transpiration (E_o). These results suggest that E_u plays a very important role in the water cycle at this site.
5. In calculating the water balance from snowmelt through the tree growth season, the total incoming water, which is the sum of precipitation (143 mm) and the water equivalent of the snow (85 mm), was 228 mm from 23 April to 19 August 2000. The

throughfall was 97 mm, and the stem flow was less than 0.1 mm. The total evapotranspiration, which is the sum of the evapotranspiration above a dry canopy for the entire ecosystem (162 mm), the interception loss (46 mm), and the understory evapotranspiration under rainy conditions, was 208-254 mm. The difference between the incoming and outgoing amounts in the water balance ranged from +20 to -26 mm.

6. Significant differences in the water and energy exchanges of the pine and larch forests at Spasskaya Pad occurred just after the snowmelt season. This could have been due to the difference in species (evergreen versus deciduous forest) or in soil thawing conditions. Consequently, the shape of the seasonal variation in the Bowen ratio over the course of the study period at the pine site was markedly different from that in the larch forest.

Acknowledgments

This study was carried out as part of GAME (GEWEX Asia Monsoon Experiment)-Siberia. The authors thank Professors T. Yasunari of Nagoya University, Y. Fukushima of the Research Institute of Humanity and Nature, and T. Ohata of Hokkaido University for their support and cooperation with the observations and analysis. We thank Professor B Ivanov, Director of the Institute for Biological Problems of the Cryolithozone, for his kind collaboration, and Associate Professor T. Tanaka of Nagoya University for his advice on the analysis. We also thank all of the members of the GAME-Siberia project for their cooperation and discussion. Finally, we thank the editor and reviewers for their useful comments and suggestions.

This study was financially supported by Grants-in-Aid of Scientific Research from the Ministry of Education, Culture, Sports, Science, and Technology of Japan (Nos.

11691124, 11201206, and 11201201), and from the Japan Society for the Promotion of Science (No. 12460063).

References

Baldocchi DD, Vogel CA, Hall B. 1997. Seasonal variation of energy and water vapor exchange rates above and below a boreal jack pine forest canopy. *Journal of Geophysical Research* **102(D24)**: 28,939-28,951.

Betts AK, Ball JH, Beljaars ACM, Miller MJ, Viterbo P. 1996. The land-surface-atmosphere interaction: a review based on observational and global modeling perspectives. *Journal of Geophysical Research* **101**: 7209-7225.

Blanken PD, Black TA, Yang PC, Neumann HH, Nesic Z, Staebler R, den Hartog G, Novak MD, Lee X. 1997. Energy balance and canopy conductance of a boreal aspen forest: Partitioning overstory and understory components. *Journal of Geophysical Research* **102(D24)**: 28,915-28,927

Bosveld FC, Bouten W. 2001. Evaluation of transpiration models with observations over a Douglas-fir forest. *Agricultural and Forest Meteorology* **108**: 247-264.

Cienciala E, Kucera J, Lindroth A. 1999. Long-term measurements of water uptake in a Swedish boreal forest. *Agricultural and Forest Meteorology* **98-99**: 547-554.

Halldin S, Gryning SE, Gottschalk L, Jochum A, Lundin LC, Van de Griend AA. 1999. Energy, water and carbon exchange in a boreal forest landscape-NOPEX experiences. *Agricultural and Forest Meteorology* **98-99**: 5-29.

Hattori S, Tamai K, Abe T. 1993. Effects of soil moisture and vapor pressure deficit on evapotranspiration in a hinoki plantation. *Journal of the Japanese Forestry Society* **75**: 216-224 [In Japanese with an English summary].

Horst TW, Weil JC. 1992. Footprint estimation for scalar flux measurements in the atmospheric surface layer. *Boundary Layer Meteorology* **59**: 279-296.

Horst TW, Weil JC. 1994. How far is far enough?: The fetch requirements for

micrometeorological measurement of surface fluxes. *Journal of Atmospheric and Oceanic Technology* **11**: 1018-1025.

Kelliher FM, Hollinger DY, Schulze ED, Vygodskaya NN, Byers JN, Hunt JE, McSeveny TM, Milukova I, Sogatchev A, Varlargin A, Ziegler W, Arneth A, Bauer G. 1997. Evaporation from an eastern Siberian larch forest. *Agricultural and Forest Meteorology* **85**: 135-147.

Kelliher FM, Lloyd J, Arneth A, Byers JN, McSeveny TM, Milukova I, Grigoriev S, Panfyorov M, Sogatchev A, Varlargin A, Ziegler W, Bauer G, Schulze ED. 1998. Evaporation from a central Siberian pine forest. *Journal of Hydrology* **205**: 279-296.

Kimball BA, Jackson RD. 1975. Soil heat flux determination: A null-alignment method. *Agricultural and Forest Meteorology* **15**:1-9.

Larsen JA. 1980. *The Boreal Ecosystem*. Academic Press. New York, USA: 35-37.

Lee X, Black TA. 1993. Atmospheric turbulence within and above a Douglas-fir stand. Part Ⅱ: Eddy fluxes of sensible heat and water vapour. *Boundary-Layer Meteorology* **64**: 369-389.

Marshall DC. 1958. Measurement of sap flow in conifers by heat transport. *Plant Physiology* **33**: 385-396

Ohta T, Hiyama T, Tanaka H, Kuwada T, Maximov TC, Ohata T, Fukushima Y. 2001a. Seasonal variation in the energy and water exchanges above and below a larch forest in eastern Siberia. *Hydrological Processes* **15** : 1459-1476.

Ohta T, Hiyama T, Maximov TC. 2001b. Preliminary observations of water and energy cycles at Spasskaya Pad, Eastern Siberia. *Proceedings of GAME-Siberia Workshop*: 3-5.

Roberts J, Pitman RM, Wallace JS. 1982. A comparison of evaporation from stands of Scots pine and Corsican pine in Thetford Chace, East Anglia. *Journal of Applied Ecology* **19**: 859-872.

Roberts J. 1983. Forest transpiration: A conservative hydrological process? *Journal of Hydrology* **66**: 133-141.

Sellers PJ, Hall FG, Margolis H, Kelly B, Baldocchi DD, Hartog G, Cihlar J, Ryan MG, Goodison B, Grill P, Ranson KJ, Lettenmaier DJ, Wickland DE. 1995. The Boreal Ecosystem-Atmosphere Study (BOREAS): an overview and early results from the 1994 field year. *Bulletin of The American Meteorological Society* **76**: 1549-1577.

Sellers PJ, Hall FG, Kelly RD, Black A, Baldocchi D, Berry J, Ryan M, Ramson KJ, Crill PM, Lettenmainer DP, Margolis H, Cihlar J, Newcomer J, Fitzjarrald D, Jarvis PG, Gower ST, Halliwell D, Williams D, Doodison B, Wickland DE, Guertin FE. 1997. BOREAS in 1997: Experiment overview, scientific results, and future directions. *Journal of Geophysical Research* **102(D24)**: 28,731-28,769.

Tamai K, Hattori S, Goto Y. 1996. Seasonal course of evapotranspiration in a deciduous broad-leaved secondary forest. *Journal of the Japan Society of Hydrology & Water Resources* **9**: 351-357 [In Japanese with an English summary].

Toba T, Ohta T. 2001. Modeling the characteristics of interception loss in forests. *Proceedings of the Fifth International Study Conference on GEWEX in Asia and GAME* **1**: 181-183.

Toba T, Ohta T. 2002. in press. Modeling the characteristics of interception loss in forests. *Journal of the Japan Society of Hydrology & Water Resources* **15**: 345-361 [In Japanese with an English summary].

Figure and Table Captions

Figure 1. Location map of the study site.

Figure 2. Crown projection diagram for (a) the pine site and (b) the larch site. The star indicates the location of the observation tower. The dots and circles indicate the positions of trunks and the canopy spread, respectively. Only the trunks' positions are shown for trees with a *DBH* smaller than 60 mm. Dark color shows the understory vegetation, *Vaccinium uva ursi*.

Figure 3. Seasonal variation in (a) precipitation, (b) air temperature, (c) specific humidity, (d) wind speed, and (e) shortwave radiation at heights of 18.2 and 1.4 m.

Figure 4. The correlation between the upwind distance and frequency distribution in the flux footprint: (a) the maximum frequency distribution and (b) the addition frequency distribution of source area distances. The atmospheric conditions on the 8 and 10 July were unstable, while they were neutral on 20 June.

Figure 5. Comparison of the sum of the turbulent fluxes ($H+\lambda E$) and the available energy flux (R_n-G).

Figure 6. Correlation between the energy imbalance (($H+\lambda E$)-(R_n-G)) and the (a) latent (λE) and (b) sensible (H) heat fluxes.

Figure 7. (a) Relationship between wind direction and the energy imbalance (($H+\lambda E$)-(R_n-G)) or the closure rate (($H+\lambda E$)/(R_n-G)). (b) Relationship between wind direction and the sensible (H) and latent (λE) heat fluxes. The error bar gives the 95% confidence intervals.

Figure 8. The seasonal variation in (a) the Bowen ratio and (b) the heat balance

exponent. R_n: net all-wave radiation, λE: latent heat flux, H: sensible heat flux, G: soil heat flux, P: precipitation.

Figure 9. Time series for (a) suction (ψ) in the soil layer, (b) atmospheric saturation deficit, and (c) the heat balance exponent. R_n: net all-wave radiation, λE: latent heat flux, H: sensible heat flux.

Figure 10. Seasonal variation in evapotranspiration. E_t: Evapotranspiration for the entire ecosystem, E_o: overstory transpiration, E_u: understory evapotranspiration, P: precipitation.

Figure 11. Daily evapotranspiration from the whole ecosystem (E_t) versus the sum of overstory transpiration (E_o) and understory evapotranspiration (E_u). The data for the larch forest in Spasskaya Pad were provided by Ohta *et al*. (2001a).

Figure 12. Correlations between overstory transpiration (E_o) (solid line), understory evapotranspiration (E_u) (dashed line), and evapotranspiration from the entire ecosystem (E_t).

Figure 13. Monthly evapotranspiration under a dry canopy (E_d) and the sum of E_d and evapotranspiration under a wet canopy (E_w).

Figure 14. Time-series for the (a) daily net all-wave radiation and ground heat flow, (b) the sensible heat flux and the latent heat flux, and (c) the Bowen ratio. The energy balance components and the Bowen ratio in this figure are for a dry canopy only (Ohta *et al*., 2001a).

Table 1. Evapotranspiration values from six studies.

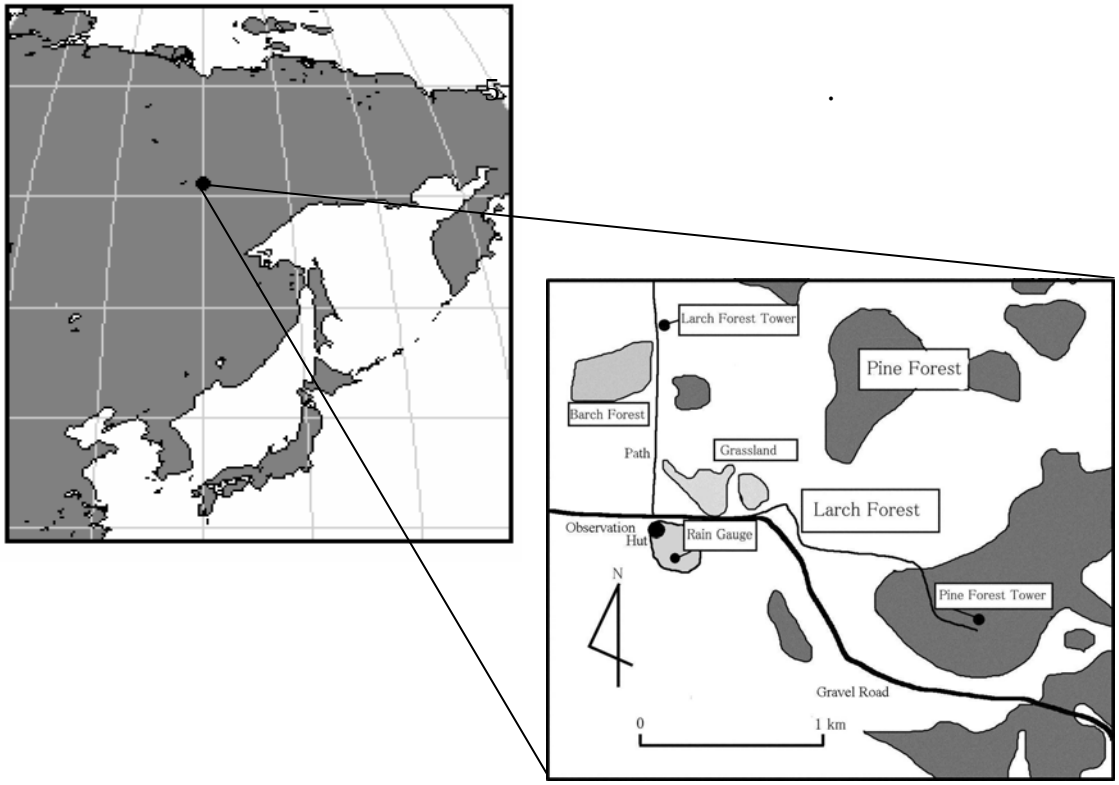

Figure 1. Location of the study site

25

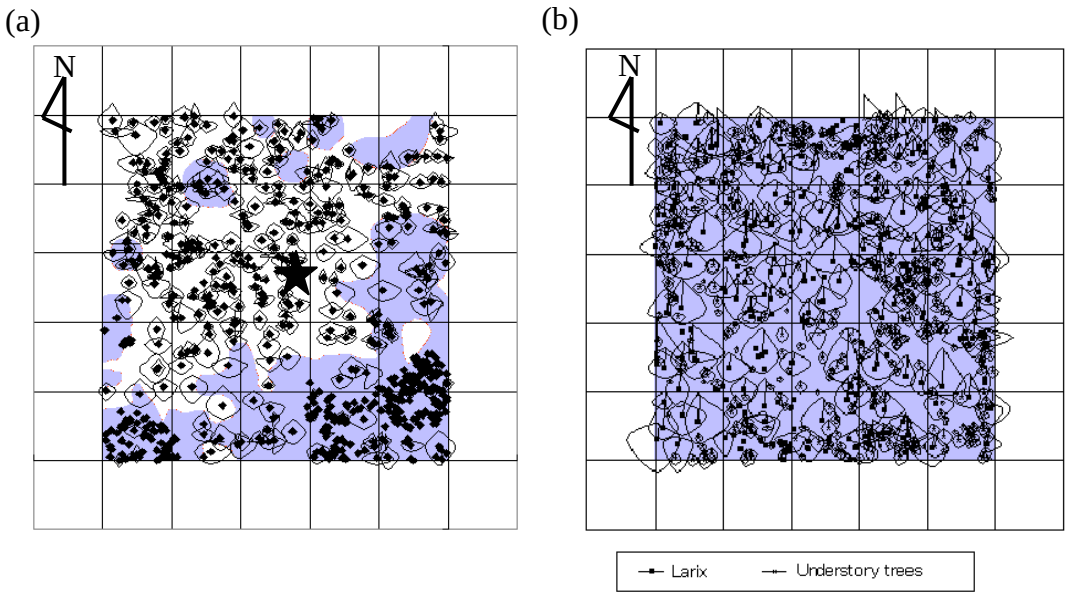

Figure 2. Crown projection diagram for (a) the pine site and (b) the larch site. The star indicates the location of the observation tower. The dots and circles indicate the positions of trunks and the canopy spread, respectively. Only the trunks' positions are shown for trees with a *DBH* smaller than 60 mm. Dark color shows the understory vegetation, *Vaccinium uva ursi*.

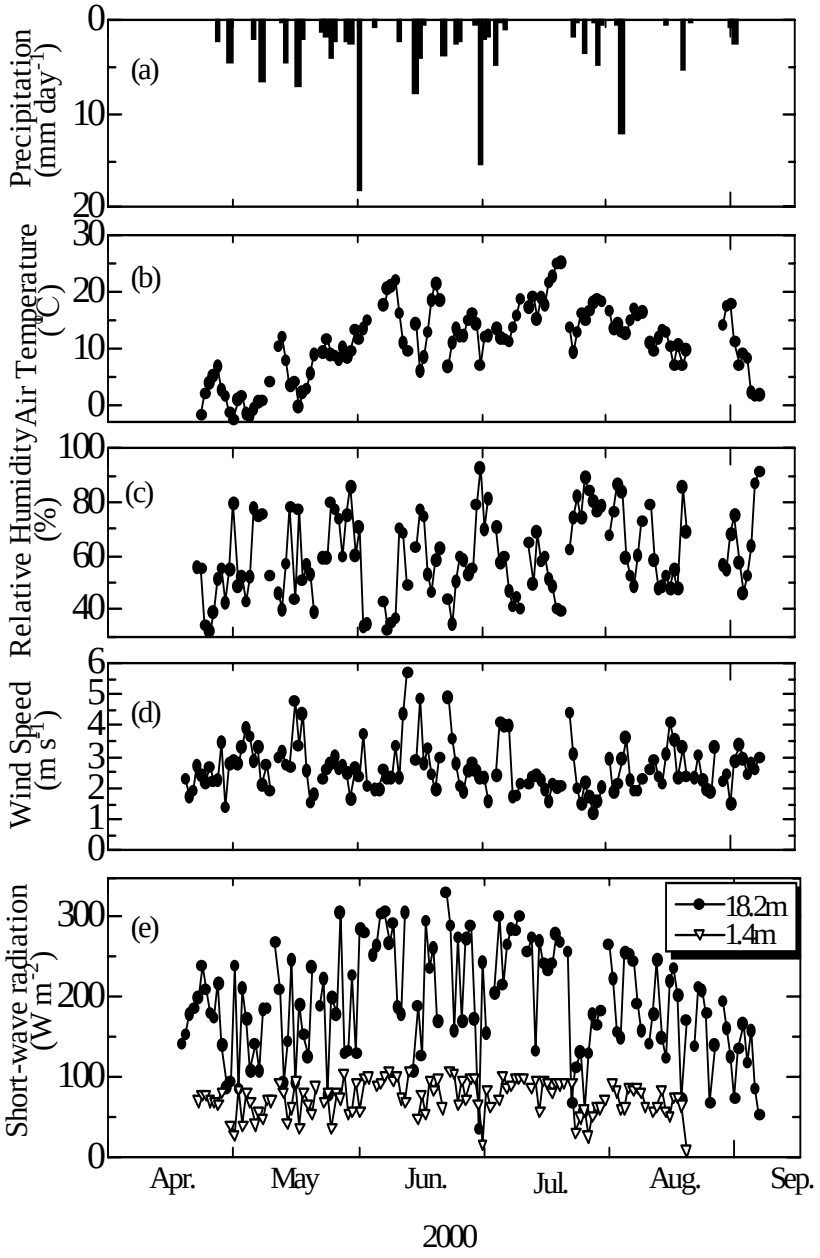

Figure 3. Seasonal variation in (a) precipitation, (b) air temperature, (c) specific humidity, (d) wind speed, and (e) shortwave radiation at heights of 18.2 and 1.4 m.

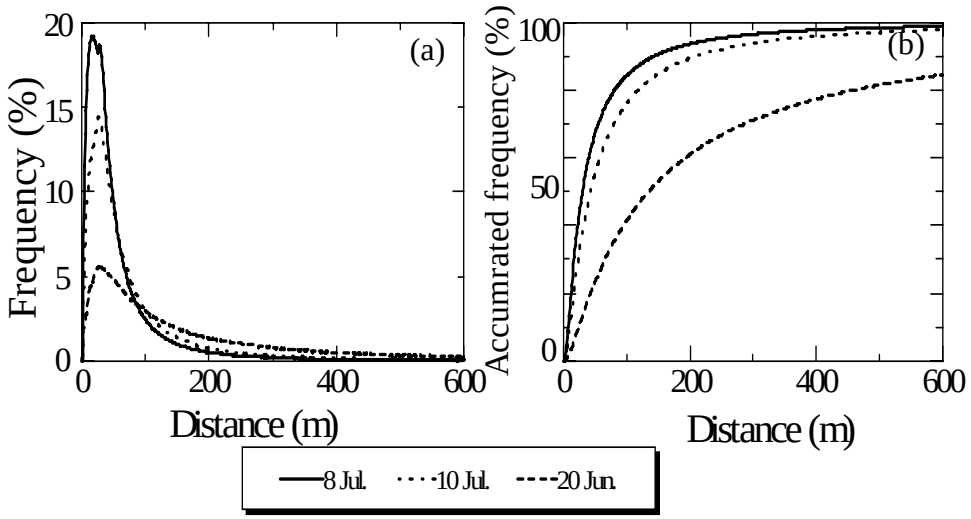

Figure 4. The correlation between the upwind distance and frequency distribution in the flux footprint: (a) the maximum frequency distribution and (b) the addition frequency distribution of source area distances. The atmospheric conditions on the 8 and 10 July were unstable, while they were neutral on 20 June.

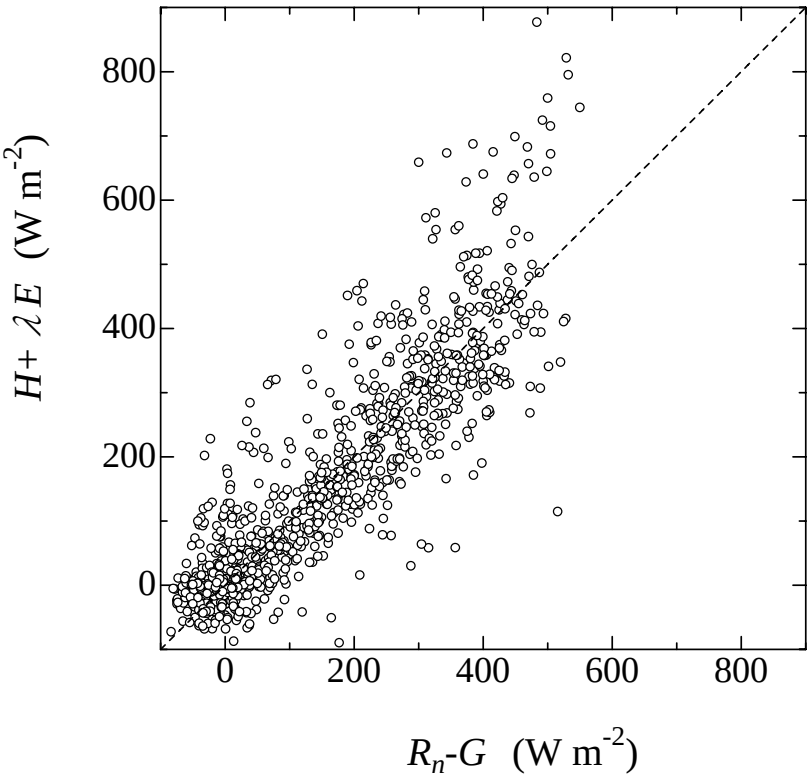

Figure 5. Comparison of the sum of the turbulent fluxes ($H+\lambda E$) and the available energy flux (R_n-G).

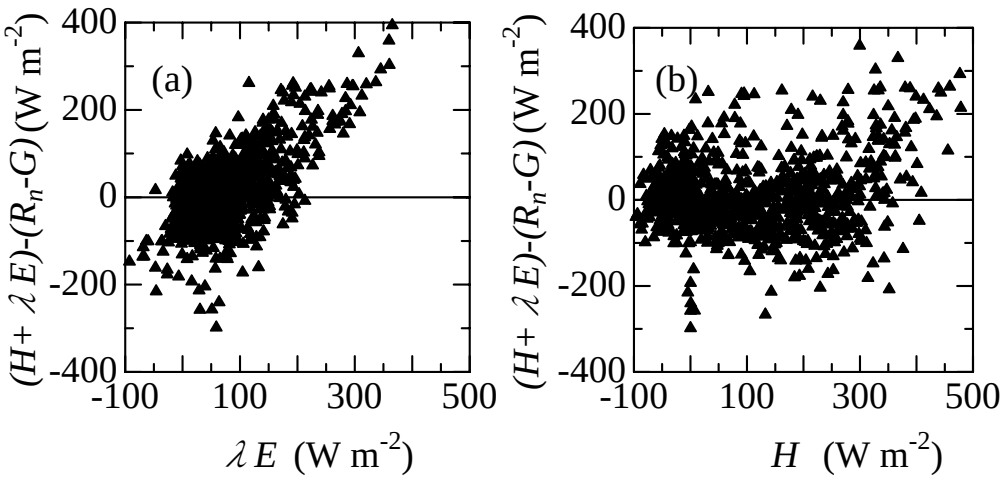

Figure 6. Correlation between the energy imbalance (($H+\lambda E$)-(R_n-G)) and the (a) latent (λE) and (b) sensible(H) heat fluxes.

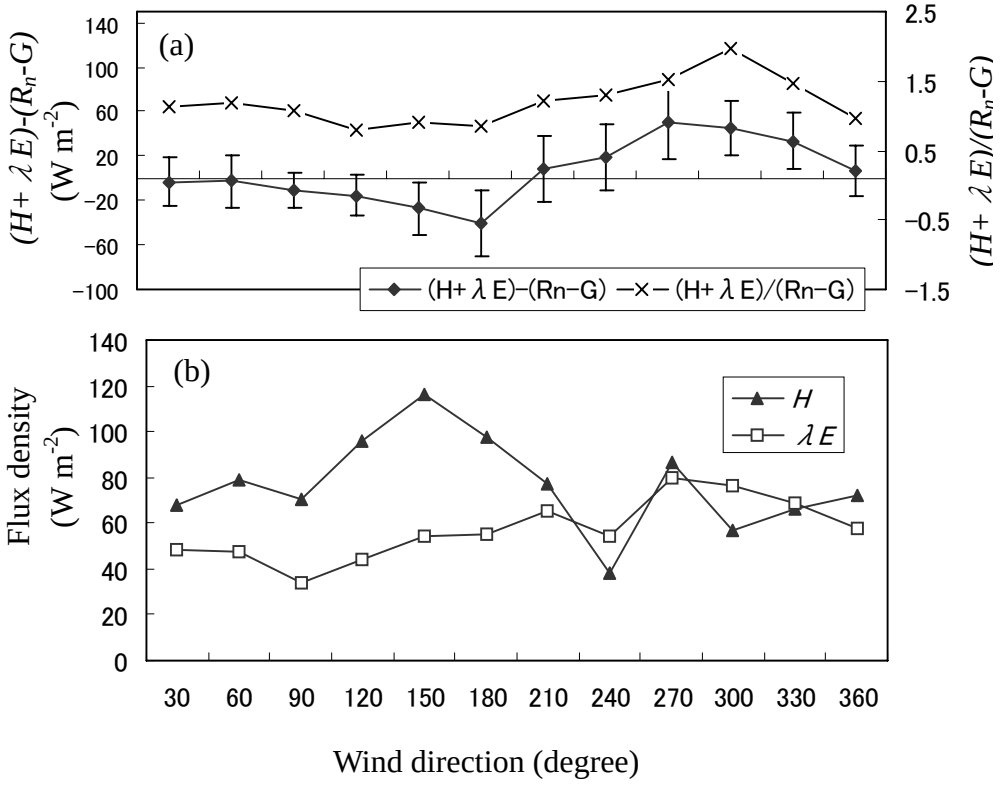

Figure 7. (a) Relationship between wind direction and the energy imbalance ($(H+\lambda E)-(R_n-G)$) or the closure rate ($(H+\lambda E)/(R_n-G)$). (b) Relationship between wind direction and the sensible (H) and latent (λE) heat fluxes. The error bar gives the 95% confidence intervals.

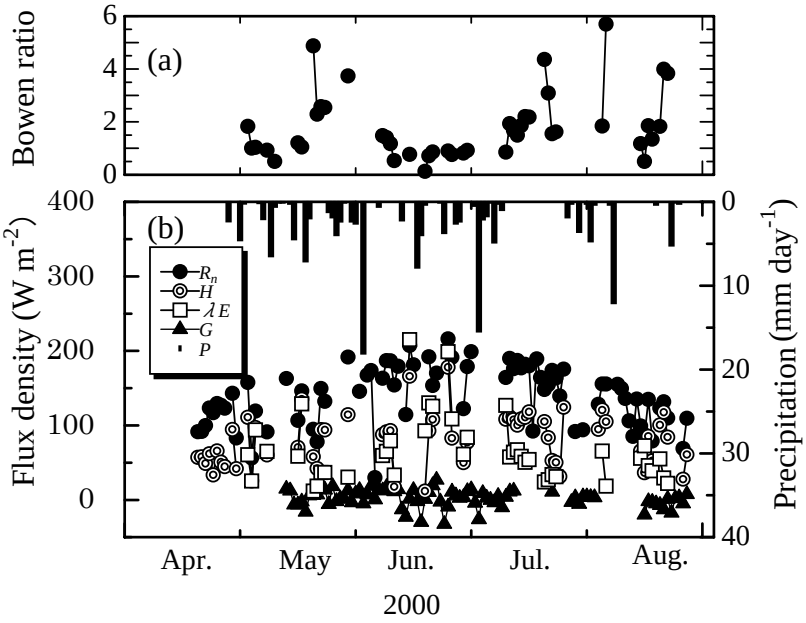

Figure 8. The seasonal variation in (a) the Bowen ratio, and (b) the heat balance exponent. R_n: net all-wave radiation, λE: latent heat flux, H: sensible heat flux, G: soil heat flux, P: precipitation.

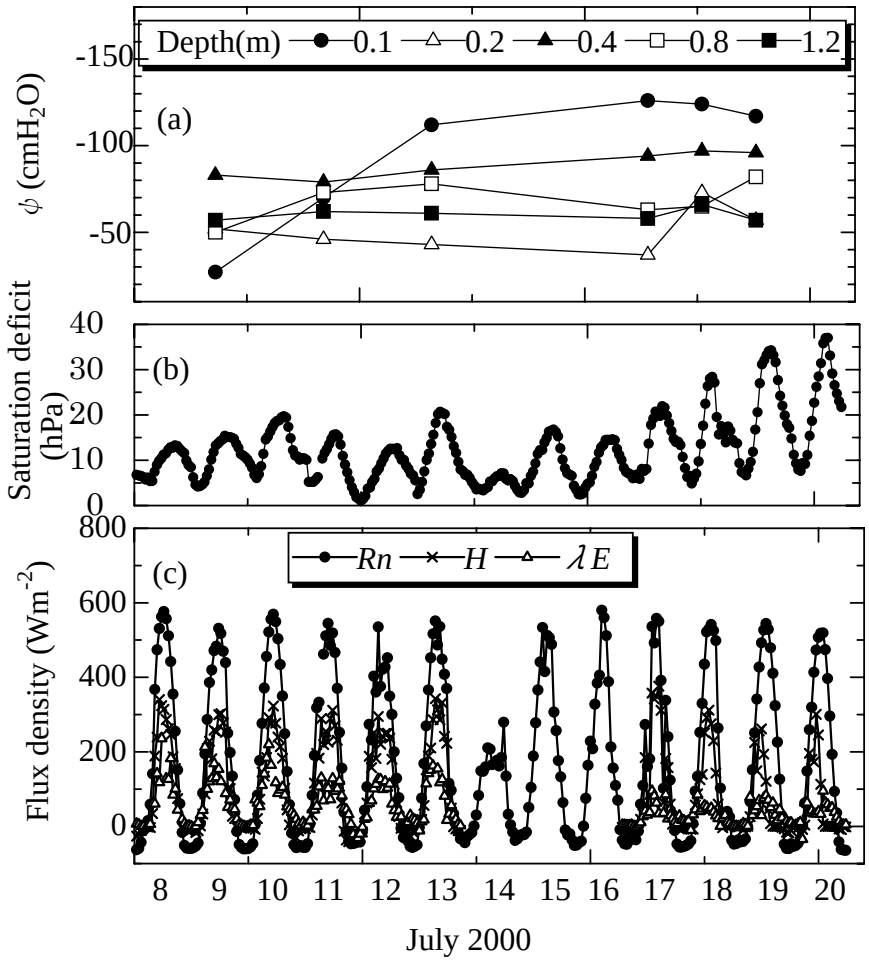

Figure 9. Time series for (a) suction (ψ) in the soil layer, (b) atmospheric saturation deficit, and (c) the heat balance exponent. R_n: net all-wave radiation, λE: latent heat flux, H: sensible heat flux.

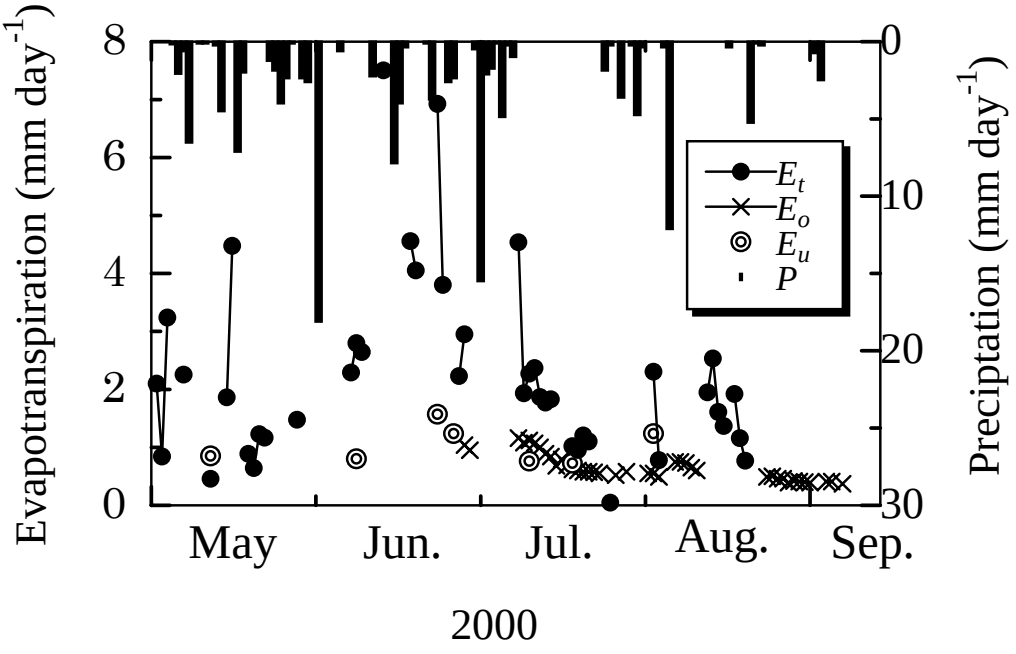

Figure 10. Seasonal variation in evapotranspiration. E_t: Evapotranspiration for the entire ecosystem, E_o: overstory transpiration, E_u: understory evapotranspiration, P: precipitation.

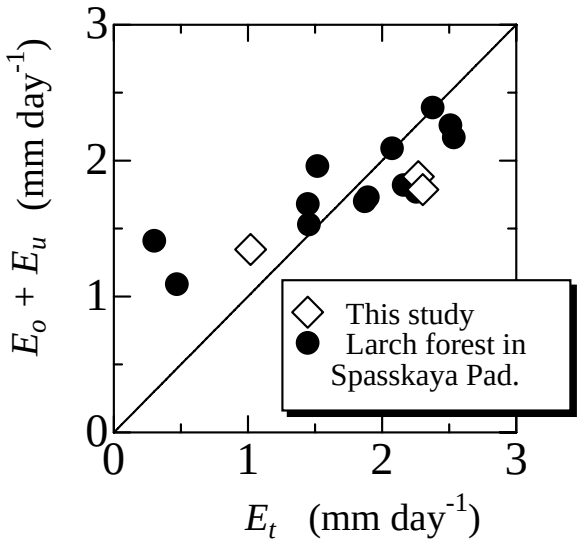

Figure 11. Daily evapotranspiration from the whole ecosystem (E_t) versus the sum of overstory transpiration (E_o) and understory evapotranspiration (E_u). The data for the larch forest at Spasskaya Pad were provided by Ohta *et al*. (2001a).

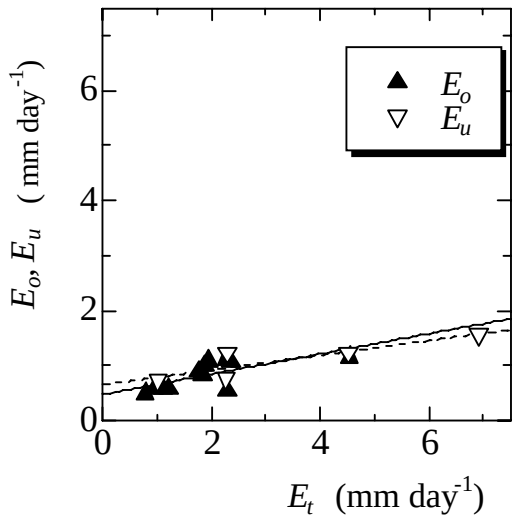

Figure 12. Correlations between overstory transpiration (E_o) (solid line), understory evapotranspiration (E_u) (dashed line), and evapotranspiration from the entire ecosystem (E_t).

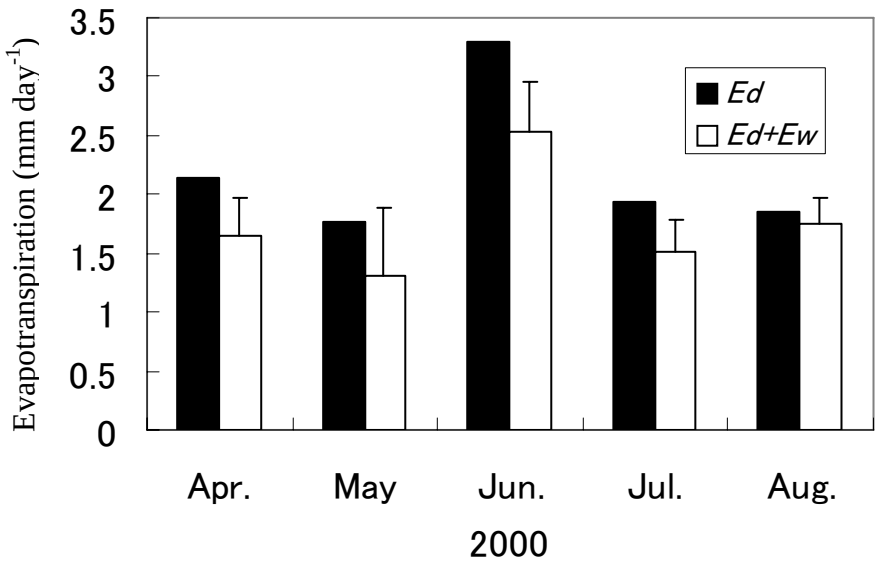

Figure 13. Monthly evapotranspiration under a dry canopy (E_d) and the sum of E_d and evapotranspiration under a wet canopy (E_w).

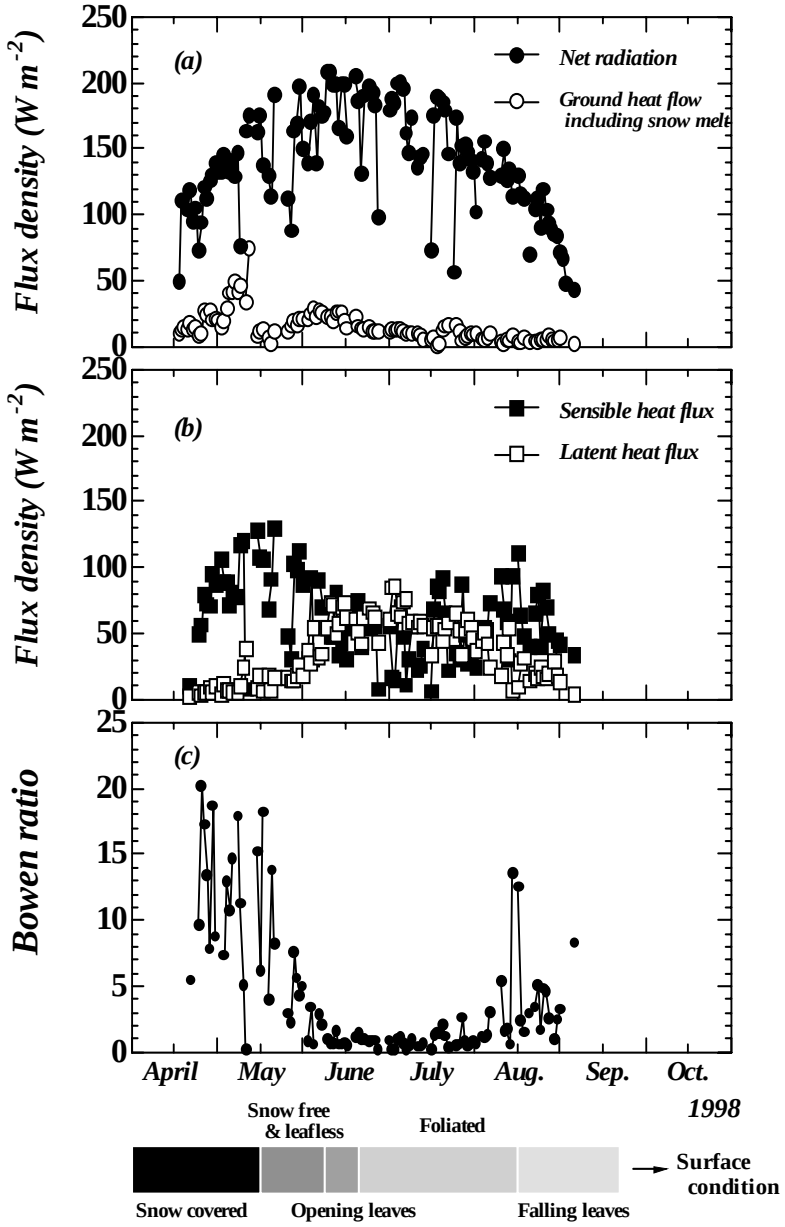

Figure 14. Time-series for the (a) daily net all-wave radiation and ground heat flow, (b) the sensible heat flux and the latent heat flux, and (c) the Bowen ratio. The energy balance components and the Bowen ratio in this figure are for a dry canopy only (Ohta *et al*., 2001a).

Table 1. Values of evapotranspiration from six studies.

No.	Vegetation	Site	Evapotranspiration ($mm\ day^{-1}$)	Period
1	*Pinus sylvestris*	Yakutsk (62° 14'N, 129° 39'E)	1.7	1, Jul.- 18, Aug., 2000
2	*Larix gmelinii*	Yakutsk (62° 5'N, 129° 45'E)	1.5	1, Jul.- 31, Aug., 1998
3	*Larix gmelinii*	Yakutsk (61°N, 128°E)	1.9	14- 27, Jul.,1993
4	*Pinus sylvestris*	Zotino (61°N, 89°E)	1.7	
5	Japanese cypress forest	Kyoto (34° 55'N, 135° 45'E)	3.4	Jul., 1991
6	Japanese deciduous forest	Kyoto (34° 47'N, 135° 51'E)	3.1	Jul., Aug.,1992

1.This study, 2.Ohta et al.(2001) 3.Kelliher et al.(1997), 4.Keliher et al.(1998), 5.Hattori et al.(1993), 6.Tamai et al.(1996)